Science of the Total Environment 773 (2021) 145630

Contents lists available at ScienceDirect

Science of the Total Environment

journal homepage: www.elsevier.com/locate/scitotenv

Edaphic variables are better indicators of soil microbial functional structure than plant-related ones in subtropical broad-leaved forests

Jingmin Cheng [a,b,c], Zhongjie Han [d], Jing Cong [e], Jingjing Yu [a], Jizhong Zhou [c,f,g], Mengxin Zhao [a,b,*], Yuguang Zhang [a,**]

[a] Research Institute of Forest Ecology, Environment and Protection, Key Laboratory of Biological Conservation of National Forestry and Grassland Administration, Chinese Academy of Forestry, Beijing 100091, China
[b] State Key Laboratory for Biology of Plant Diseases and Insect Pests, Institute of Plant Protection, Chinese Academy of Agricultural Sciences, Beijing 100193, China
[c] State Key Joint Laboratory of Environment Simulation and Pollution Control, School of Environment, Tsinghua University, Beijing 100084, China
[d] Faculty of Environmental and Life Sciences, Beijing University of Technology, Beijing 100124, China
[e] College of Marine Science and Biological Engineering, Qingdao University of Science and Technology, Qingdao 266042, China
[f] Institute for Environmental Genomics and Department of Microbiology and Plant Biology, University of Oklahoma, Norman, OK 73019, USA
[g] Earth Sciences Division, Lawrence Berkeley National Laboratory, Berkeley, CA 94720, USA

HIGHLIGHTS

- Soil microbial functional structure differs among SBFs.
- The MBF has the highest soil microbial functional α-diversity but the lowest functional β-diversity.
- The MBF has the highest functional capabilities in nutrient cycling processes.
- Edaphic variables are more correlated with soil microbial functional structure than plant-related ones in SBFs.

GRAPHICAL ABSTRACT

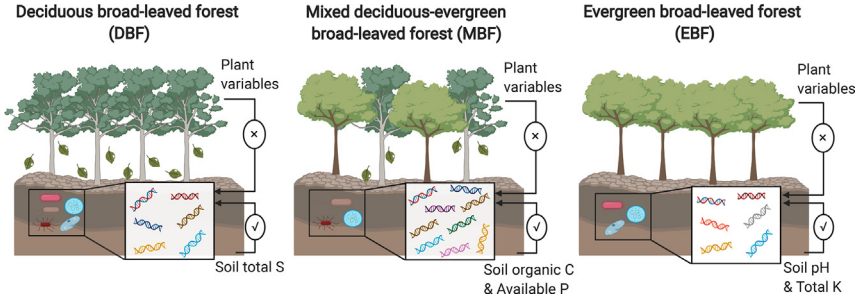

ARTICLE INFO

Article history:
Received 8 October 2020
Received in revised form 25 January 2021
Accepted 31 January 2021
Available online 6 February 2021

Editor: Yucheng Feng

Keywords:
Environmental variables
Network analyses
Functional genes
GeoChip
Subtropical broad-leaved forests

ABSTRACT

Soil microorganisms play important roles in the ecosystem functioning of subtropical broad-leaved forests (SBFs). However, the patterns and environmental indicators of soil microbial functional structure remain unclear in SBFs. In the present work, we used a functional microarray (GeoChip 4.0) to examine the soil microbial functional structure of three types of SBFs, including a deciduous broad-leaved forest (DBF), a mixed evergreen-deciduous broad-leaved forest (MBF), and an evergreen broad-leaved forest (EBF). We found that microbial functional structure was significantly different among SBFs ($P < 0.05$). Compared to the DBF and the EBF, the MBF had higher functional α-diversity ($P = 0.001$, $F = 12.55$) but lower β-diversity ($P < 0.001$, $F = 61.09$), and showed more complex functional gene networks. Besides, the MBF had higher relative abundances of functional genes for carbon (C) decomposition, C fixation, nitrogen (N) cycling, sulfur (S) cycling, and phosphorus (P) cycling ($P < 0.05$), indicating stronger microbial functional capabilities of nutrient cycling processes. Edaphic variables (i.e., soil pH and soil nutrient content) were revealed as better indicators of soil microbial functional structure than plant-related ones (i.e., vegetation type and plant diversity) in SBFs. For example, functional gene structure of the DBF was significantly related to soil total S ($P = 0.041$), that of the MBF was significantly related to soil organic C ($P = 0.027$) and plant available P ($P = 0.034$), and that of the EBF was significantly

* Correspondence to: M. Zhao, State Key Laboratory for Biology of Plant Diseases and Insect Pests, Institute of Plant Protection, Chinese Academy of Agricultural Sciences, Beijing 100193, China.
** Correspondence to: Y. Zhang, Research Institute of Forest Ecology, Environment and Protection, and the Key Laboratory of Biological Conservation of National Forestry and Grassland Administration, Chinese Academy of Forestry, Beijing 100091, China.
E-mail addresses: chengjm17@mails.tsinghua.edu.cn (J. Cheng), zhongjiehan@emails.bjut.edu.cn (Z. Han), yqdh77@163.com (J. Cong), 15034576002@163.com (J. Yu), jzhou@ou.edu (J. Zhou), zhaomengxin11@tsinghua.org.cn (M. Zhao), yugzhang@sina.com.cn (Y. Zhang).

https://doi.org/10.1016/j.scitotenv.2021.145630
0048-9697/

related to soil pH ($P = 0.006$) and total potassium (K) ($P = 0.038$). Overall, through the analysis of microbial functional gene profiles, this study yields unique insights into the environmental indicators of patterns and mechanisms of soil microbial functional structure in SBFs.

1. Introduction

Soil microorganisms play important roles in ecosystem functioning including organic carbon (C) decomposition (De Graaff et al., 2010), C fixation (Lynn et al., 2017), nitrogen (N) cycling (Harter et al., 2014), phosphorus (P) cycling (Dai et al., 2020), sulfur (S) cycling (Ulrich et al., 1998), etc. Plant-related variables and edaphic variables are commonly considered as direct or indirect indicators of soil microbial functions (Berg and Smalla, 2009). For example, higher plant diversity could increase the turnover rate of plant biomass as well as soil nutrient input, and therefore positively stimulates soil microbial functions in nutrient cycling processes (Zak et al., 2003). Besides, given that the C decomposition ability of soil microorganisms probably reflects the substrates present in the soil C pool, plant type (or plant cover composition) may also influence soil microbial functions (Chodak et al., 2015). Patterns and mechanisms of microbial functional structure are keys to understanding functional capabilities of soil microorganisms and functional variabilities of soil microhabitats (Ettema and Wardle, 2002). However, this information in subtropical broad-leaved forests (SBFs) remains limited, despite SBFs make considerable contributions to global biodiversity and nutrient cycling (Yu et al., 2014).

Generally, deciduous broad-leaved plant species and evergreen ones co-occur in SBFs, forming vegetation types including deciduous broad-leaved forests (DBFs), evergreen broad-leaved forests (EBFs), and mixed evergreen-deciduous broad-leaved forests (MBFs) (Yu et al., 2014). Associated with distinct plant properties (e.g., evergreen forests are often of poorer leaf nutrients, lower photosynthetic capacity, and a smaller specific leaf area than deciduous ones) (Antúnez et al., 2001; Pearse et al., 2014; Takashima et al., 2004), litter properties (e.g., litter quality and quantity) (Pérez-Suárez et al., 2009), and soil properties (e.g., lower root exudation rates and net N mineralization rate in evergreen forests than in deciduous ones) (Wang et al., 2021), distinct patterns of soil microbial taxonomic structure among vegetation types have also been reported (Cheng et al., 2020; Ding et al., 2015b). Although high throughput sequencing technologies have allowed for rapid characterization of microbial taxonomy, perhaps the biggest challenge at present is how to link microbial taxonomy with their ecological functions (Torsvik and Øvreås, 2002). In the last decade, functional microarrays, such as GeoChip, have been intensively used to assay functional capacities of microbial members in environmental samples (Levy-Booth et al., 2014; Ma et al., 2019; Yergeau et al., 2007; Zimmerman et al., 2016). GeoChip primarily targets microbial genes with biogeochemical functions (e.g., C, N, S, and P cycling, organic contaminant degradation, metal resistance, virulence) (He et al., 2007). As a quantitative tool of microbial functional genes, GeoChip has been particularly powerful in determining microbial functional capabilities in various natural habitats including grasslands (Wang et al., 2016), arctic tundra (Xue et al., 2016), mangroves (Bai et al., 2013), deep-sea hydrothermal vents (Wang et al., 2009), etc.

Here, we applied GeoChip to reveal the patterns and mechanisms of microbial functional structure of a DBF, a MBF, and an EBF in south-central China. Microbial functional traits including composition, diversity, relative abundance, and network topology of functional genes were compared among the three vegetation types. According to a previous study demonstrating that aboveground plant community could be a major driving force of belowground community (Lamb et al., 2011), we hypothesized that 1) patterns of soil microbial functional structure would be different among the three vegetation types, 2) the difference of soil microbial functional structure among forests could be attributed to both the aboveground plant-related variables and belowground edaphic ones, and 3) edaphic variables would be better indicators of soil microbial functional structure than plant-related ones due to GeoChip itself targets biogeochemical cycles.

2. Methods & materials

2.1. Study area

Soil samples were collected from three SBFs in south-central China, including a DBF located at the Saiwudang Natural Reserve in Hubei Province (32°25′51.29″N, 110°45′4.29″E, 1108 m above sea level), a MBF located at the Badagongshan Natural Reserve in Hunan Province (29°46′24.23″N, 110°4′26.95″E, 1453 m above sea level), and an EBF located at the Houhe National Nature Reserve in Hubei Province (30°4′43.00″N, 110°32′58.89″E, 1568 m above sea level) (Fig. S1). The geographical distance between Saiwudang and Badagongshan is 652 km, and that between Saiwudang and Houhe is 516 km, and that between Badagongshan and Houhe is 183 km (Fig. S1). All the three forests were historically used as forestry farms for timber and charcoal harvesting, and have become natural restorations since deforestation was prohibited in the 1980s. The soil type of the three forests is similar, i.e., mountain yellow-brown soil. The DBF has a mean annual temperature (MAT) of 10.67 °C and a mean annual precipitation (MAP) of 1009.5 mm, dominated by *Quercus glandulifera* (Fagaceae), *Platycarya strobilacea* (Juglandaceae), and *Castanea henryi* (Fagaceae). The MBF has a MAT of 11.56 °C and a MAP of 1527.1 mm, dominated by *Carpinus chuniana* (Betulaceae), *Sorbus folgneri* (Rosaceae), and *Cyclobalanopsis multinervis* (Fagaceae). The EBF has a MAT of 11.18 °C and a MAP of 1465.6 mm, dominated by *Sycopsis sinensis* (Hamamelidaceae), *Cyclobalanopsis glauca* (Fagaceae), and *Cyclobalanopsis oxyodon* (Fagaceae).

2.2. Plant survey

A detailed description of the plant survey has been previously reported (Cheng et al., 2020). In brief, we randomly selected 9 plots (20×20 m) in each forest and identified all visible plants to the species level. For those trees with the diameter at breast height (DBH) > 5 cm, we classified them as canopy trees and measured their richness, height, and DBH to calculate the Importance Value Index (IVI) (Curtis and Mcintosh, 1951) of each canopy tree species. Each canopy tree species was determined to be either deciduous or evergreen. IVI values of all deciduous canopy tree species in a plot were summed up, and we defined the sum as "dIVI", a quantitative indicator of vegetation types. Plant richness, Shannon-Wiener index, and Pielou's evenness, were calculated based on the survey of all plant species in a plot, including canopy trees, shrubs (5 cm ≥ DBH > 1 cm), and herbs.

2.3. Soil sampling, DNA extraction & edaphic variable measurements

We collected soil samples in September 2012 before the defoliation of deciduous trees. A total of 10–15 random top-soil cores (0–10 cm) per plot were collected and thoroughly mixed as one sample. Coarse gravels and plant roots were removed using a 2 mm mesh. Soil samples were stored on ice and delivered to the laboratory for DNA extraction and edaphic variable measurements.

We extracted soil DNA using the MoBio PowerSoil DNA Isolation Kit (MoBio Laboratories, Carlsbad, CA, USA) and purified the DNA products using the Genomic DNA Clean & Concentrator Kit (Zymo Research, Irvine, CA, USA). DNA quality and concentration were measured through a NanoDrop ND-1000 Spectrophotometer (NanoDrop Technologies Inc., Wilmington, DE, USA) and a FLUOstar OPTIMA fluorescence plate reader (BMG LABTECH, Jena, Germany), respectively.

We measured a range of edaphic variables following the previously described protocols (Bao, 2000; Ding et al., 2015b), including soil pH, soil organic C, total N, total potassium (K), total S, total P, alkali-hydrolysable N, NH_4^+-N, NO_3^--N, plant available P, and Fe^{3+}.

2.4. GeoChip 4.0 hybridization

GeoChip 4.0 (NimbleGen, Madison, WI, USA) was used to investigate microbial functional structure, which contains 83,992 oligonucleotide probes (50-mer) targeting 410 gene categories in association with the biogeochemical cycling of C, N, P, and S, organic contaminants, stress, virulence, etc. (Lu et al., 2012). For each sample, 1 μg of DNA was labeled with Cy5 fluorescent dye (GE Healthcare, Madison, WI, USA) and hybridized with GeoChip microarrays at 45 °C for 10 h. Unbounded DNA was washed away. GeoChip microarrays were scanned by a NimbleGen MS 200 Microarray Scanner (Roche, Basel, Switzerland). Signal intensities were measured using ImaGene 6.0 (Biodiscovery, El Segundo, CA), and only those with a signal-to-noise ratio (SNR) > 2.0 [SNR = (signal intensity − background intensity) / standard deviation of the background] were used for further analyses. The following data transformation included: (1) removing genes detected in less than 3 of 9 samples in each forest; (2) dividing the signal intensity of each gene by the sum of each sample, and then multiplying it by the average of all samples; and (3) performing natural log-transformation.

2.5. Statistical analyses

Plant-related variables (including dIVI, Shannon-Wiener index, richness, and Pielou's evenness) and edaphic variables (including soil pH, total C, total N, total K, total P, total S, NH_4^+-N, NO_3^--N, alkali-hydrolysable N, plant available P, and Fe^{3+}) have been previously analyzed and published (Cheng et al., 2020). Microbial functional gene structure was visualized via the PCoA (principal coordinates analysis) plot, performed by the function '*pco*' in the R package *vegan*. Dissimilarity of microbial functional gene structure across forests was examined via three non-parametric multivariate analyses, including the multi-response permutation procedure (MRPP), the multivariate analysis of variance (Adonis), and the analysis of similarity (ANOSIM), performed by functions '*mrpp*', '*adonis2*', and '*anosim*' in *vegan*. For each non-parametric multivariate analysis, three types of dissimilarity including Bray-Curtis, Euclidean, and Horn were selected to ensure reliability. Multiple comparisons of microbial functional gene α-diversity (i.e., Shannon-Wiener index), richness (i.e., number of gene probes detected), β-diversity (i.e., variation among sampling plots within a forest), and relative abundance of functional genes across forests were carried out with Tukey HSD after the general linear model using the sampling plot as a random factor, performed by the IBM SPSS statistics software (version 23.0). *P*-values were adjusted by the Benjamini & Hochberg (BH) correction via the function '*p.adjust*' in the R package *stats*. In this study, we only focused on those microbial functional genes for nutrient cycling processes, including C decomposition genes, C fixation genes, N cycling genes, P cycling genes, and S cycling genes. Linkages between microbial functional gene structure and environmental variables (including plant-related ones and edaphic ones) were detected by partial Mantel tests using the function '*mantel.partial*' in *vegan*. Moreover, to estimate the relative importance of plant-related variables and edaphic variables, we conducted the MRM (multiple regression on distance matrices) using the function '*MRM*' in the R package *ecodist*. Before performing the partial Mantel test and MRM, environmental variables were transformed via the function '*scale*' in the R package *base*.

2.6. Network construction

To estimate potential interactions among functional genes or microorganisms containing those genes (Zhou et al., 2011), we constructed molecule ecological networks using the microbial functional gene data. Forest-specific networks of genes for C decomposition, C fixation, N cycling, P cycling, and S cycling were constructed separately. Network construction was based on the Random Matrix Theory (RMT) algorithm, via the pipeline of Molecular Ecological Network Analyses (MENA) (http://ieg4.rccc.ou.edu/mena/) (Deng et al., 2012; Zhou et al., 2011). For the C decomposition networks, not all genes were included for network construction, because the data table uploaded to MENA should be less than 5,000 rows. Since we detected a total of 7,243 gene probes for C decomposition, which exceeded the maximum row number of MENA, we selected the top 10 abundant genes for network construction, including the endoglucanase gene, chitinase gene, ligninase gene, *amyA*, cellobiase gene, phenol oxidase gene, endochitinase gene, exoglucanase gene, exochitinase gene, and xylanase gene. The top 10 abundant genes had 4,022 probes in total (i.e., row number = 4,022). For the C fixation, N cycling, P cycling, and S cycling networks, all genes were included for network construction. Overall network topological characteristics including threshold (i.e., the minimum Spearman's correlation coefficient between pairwise functional genes for network construction), total nodes, total edges, R^2 of power-law, average connectivity, average clustering coefficient, and modularity were calculated via MENA. Thresholds for network construction were automatically identified by MENA: Briefly, RMT identified the transition points from Gaussian orthogonal ensemble statistics to Poisson distribution and used the transition points as thresholds (Deng et al., 2012). To compare network topological characteristics among vegetation types, we chose the same threshold from RMT-identified transition points to construct forest-specific networks. Cytoscape (version 3.8.0) was used to visualize network topology.

3. Results

3.1. Plant-related and edaphic variables

According to our previous work (Cheng et al., 2020), the DBF and the MBF exhibited a higher plant Shannon-Wiener index than the EBF. The EBF exhibited higher soil pH than the DBF and the EBF. Compared to the MBF and the EBF, the DBF exhibited higher plant available P but lower soil organic C, total N, total P, total S, NO_3^--N, and Fe^{3+} (see Table S1 for more information).

3.2. Patterns of soil microbial functional structure

A total of 23,820 probes of 345 functional genes were detected from the overall 27 soil samples, among which 60 genes were in association with C decomposition, 56 genes with C fixation, 20 genes with N cycling, 3 genes with P cycling, and 15 genes with S cycling. In line with our Hypothesis 1, we found significantly different patterns of functional gene structure among the three forests (Table 1, $P < 0.05$; Fig. 1a). Compared to the DBF (10.02) and the EBF (10.03), the MBF (10.06) exhibited significantly higher functional α-diversity (Fig. 1b, $P = 0.001$, $F = 12.55$). Besides, the MBF exhibited significantly higher gene richness (DBF: 22,833; MBF: 23,124; EBF: 23,576) (Fig. 1c, $P = 0.001$, $F = 11.76$) but significantly lower functional β-diversity (DBF: 0.037; MBF: 0.019; EBF: 0.028) (Fig. 1d, $P < 0.001$, $F = 61.09$).

3.2.1. C decomposition genes

Significant difference of C decomposition genes was observed among forests ($P < 0.001$, $F = 25.53$). For example, genes for relatively

Table 1
Dissimilarity test results of microbial functional gene composition between each pair of forests. Dissimilarity tests include the multi-response permutation procedure (MRPP), the non-parametric multivariate analysis of variance (Adonis), and the analysis of similarity (ANOSIM). DBF: the deciduous broad-leaved forest. MBF: the mixed deciduous-evergreen broad-leaved forest. EBF: the evergreen broad-leaved forest. Bold values indicate significance at the $P < 0.01$ level.

	Distance method	MRPP		Adonis		ANOSIM	
		δ	*P*	F	*P*	R	*P*
DBF vs. MBF	Bray-Curtis	0.028	**0.001**	5.786	**0.001**	0.457	**0.001**
	Euclidean	195.400	**0.001**	5.786	**0.002**	0.248	**0.001**
	Horn	0.014	**0.002**	5.786	**0.001**	0.220	**0.001**
DBF vs. EBF	Bray-Curtis	0.327	**0.001**	3.048	**0.001**	0.351	**0.001**
	Euclidean	230.200	**0.003**	3.048	**0.001**	0.157	**0.003**
	Horn	0.019	**0.007**	3.048	**0.001**	0.148	**0.001**
MBF vs. EBF	Bray-Curtis	0.024	**0.001**	7.625	**0.001**	0.574	**0.001**
	Euclidean	178.100	**0.001**	7.625	**0.001**	0.239	**0.001**
	Horn	0.011	**0.001**	7.625	**0.001**	0.226	**0.001**

labile C decomposition including starch decomposition (the *amyA* encoding α-amylase), hemicelluloses decomposition gene (the xylanase gene), cellulose decomposition genes (the cellobiase gene, the endoglucanase gene, and the exoglucanase gene) were more abundant in the MBF than in the DBF and the EBF (Fig. 2, $P < 0.05$). In addition, genes for the decomposition of relatively recalcitrant C, e.g., the chitinase gene and the endochitinase gene for chitin decomposition, the phenol oxidase gene for lignin decomposition were also more abundant in the MBF (Fig. 2, $P < 0.05$). Among the three forests, relative abundances of *amyA*, endoglucanase gene, and phenol oxidase gene were the lowest in the DBF (Fig. 2, $P < 0.05$).

3.2.2. C fixation genes

We detected significantly higher relative abundances of C fixation genes in the MBF than in other forests ($P < 0.001$, $F = 27.72$), including the carboxysome gene for enhancing C fixation efficiency, key genes involved in the Calvin cycle (such as the fructose 1, 6-bisphosphate (FBP) gene, the FBP aldolase gene, the glyceraldehyde-3-phosphate dehydrogenase (GAPDH) gene, the phosphoglycerate kinase (PGK) gene, the *rpiA* encoding ribose-5-phosphate isomerase, the ribulose-1,5-bisphosphate carboxylase/oxygenase (Rubisco) gene, the triosephosphate isomerase (TIM) gene, and the *tktA* encoding transketolase), and the key gene involved in the reductive acetyl-CoA pathway, i.e., the formyltetrahydrofolate synthetase (FTHFS) gene. Relative abundances of carboxysome gene, FBP aldolase gene, and Rubisco gene in the DBF were the lowest in the DBF (Fig. S1, $P < 0.05$).

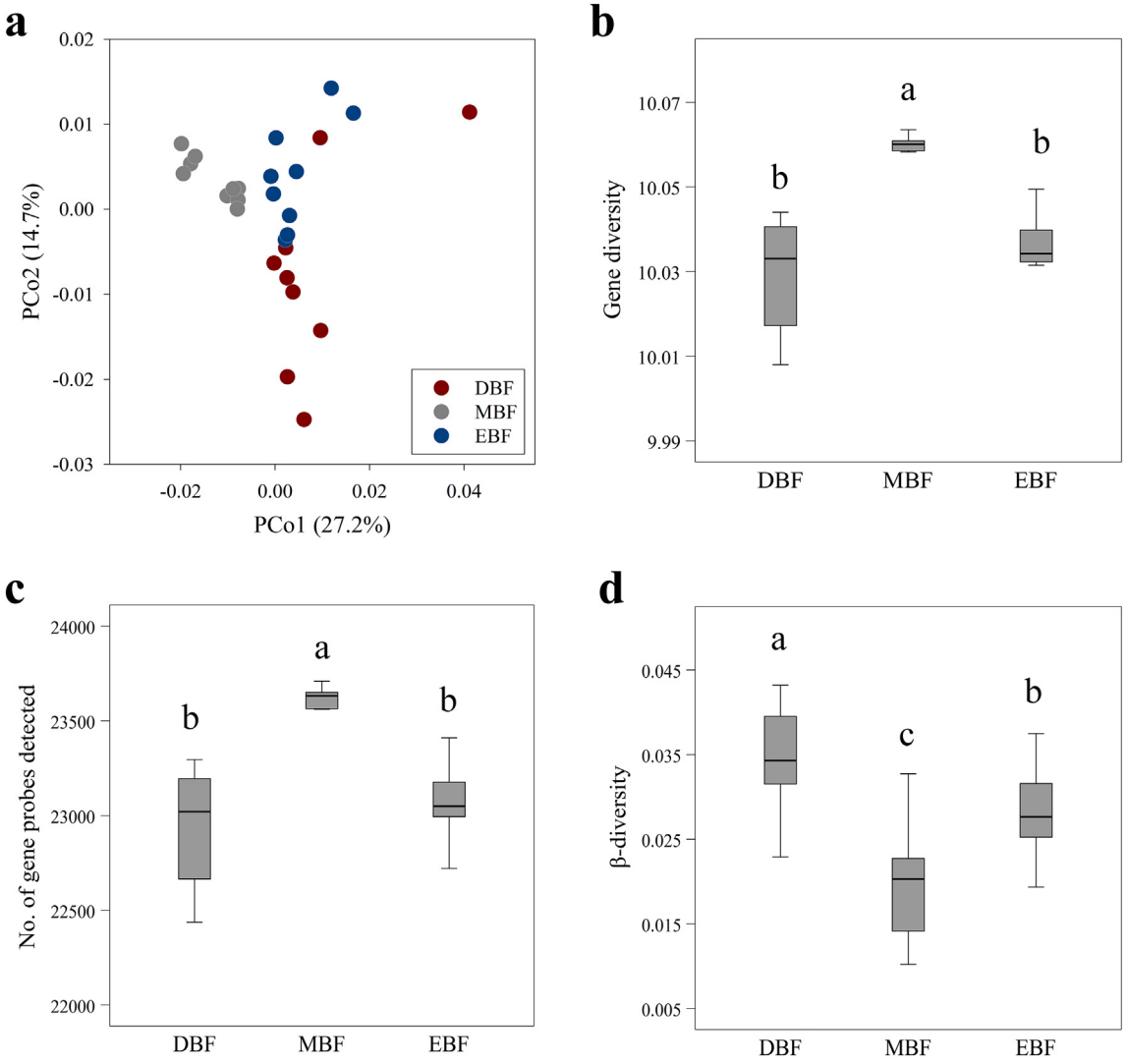

Fig. 1. (a) The PCoA (principal coordinates analysis) plot of microbial functional gene composition; **(b)** The α-diversity (i.e., Shannon-Wiener index) of microbial functional genes; **(c)** The richness (i.e., number of gene probes detected) of microbial functional genes; and **(d)** The β-diversity of microbial functional genes. DBF: the deciduous broad-leaved forest. MBF: the mixed deciduous-evergreen broad-leaved forest. EBF: the evergreen broad-leaved forest. Letters including "a" "b" and "c" above bars indicate significant difference ($P < 0.05$) among forests.

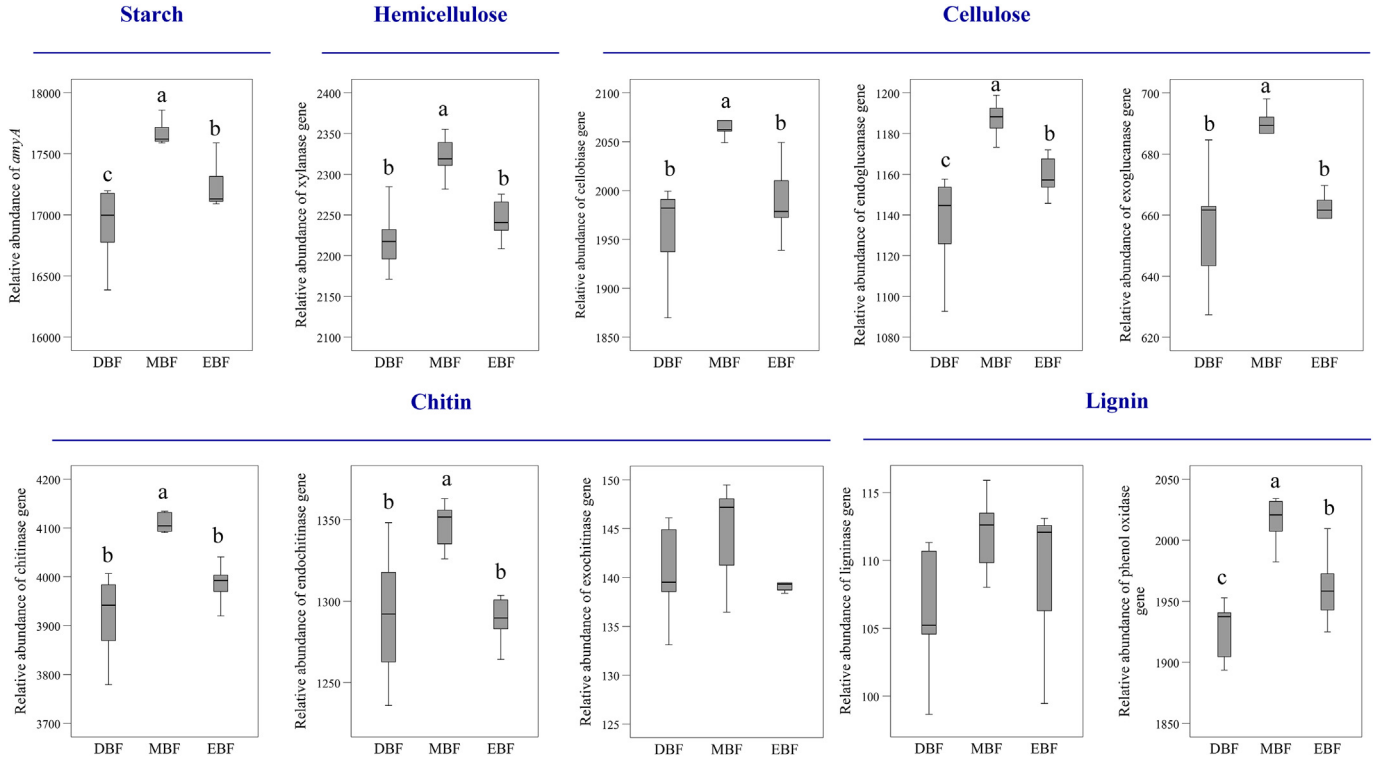

Fig. 2. Comparison of microbial functional genes for C decomposition among forests. DBF: the deciduous broad-leaved forest. MBF: the mixed deciduous-evergreen broad-leaved forest. EBF: the evergreen broad-leaved forest. Letters including "a" "b" and "c" above bars indicate significant difference ($P < 0.05$) among forests.

3.2.3. N cycling genes

Significant differences in relative abundances of N cycling genes were observed among forests ($P < 0.001$, $F = 22.67$). For example, genes for ammonification, including the *gdh* encoding glutamate dehydrogenase and the *ureC* encoding urease, were more abundant in the MBF than in the DBF and the EBF (Fig. 3, $P < 0.05$). Relative abundances of the *nirB* encoding nitrite reductase for assimilatory N reduction ($NO_2^- \rightarrow NH_4^+$), the *amoA* encoding ammonia monooxygenase for nitrification, and the *nifH* encoding nitrogenase reductase for N fixation were also significantly higher in the MBF (Fig. 3, $P < 0.05$). In addition, genes for denitrification, including the *nirK* and *nirS* encoding nitrite reductase ($NO_2^- \rightarrow NO$), as well as the *nosZ* encoding nitrous

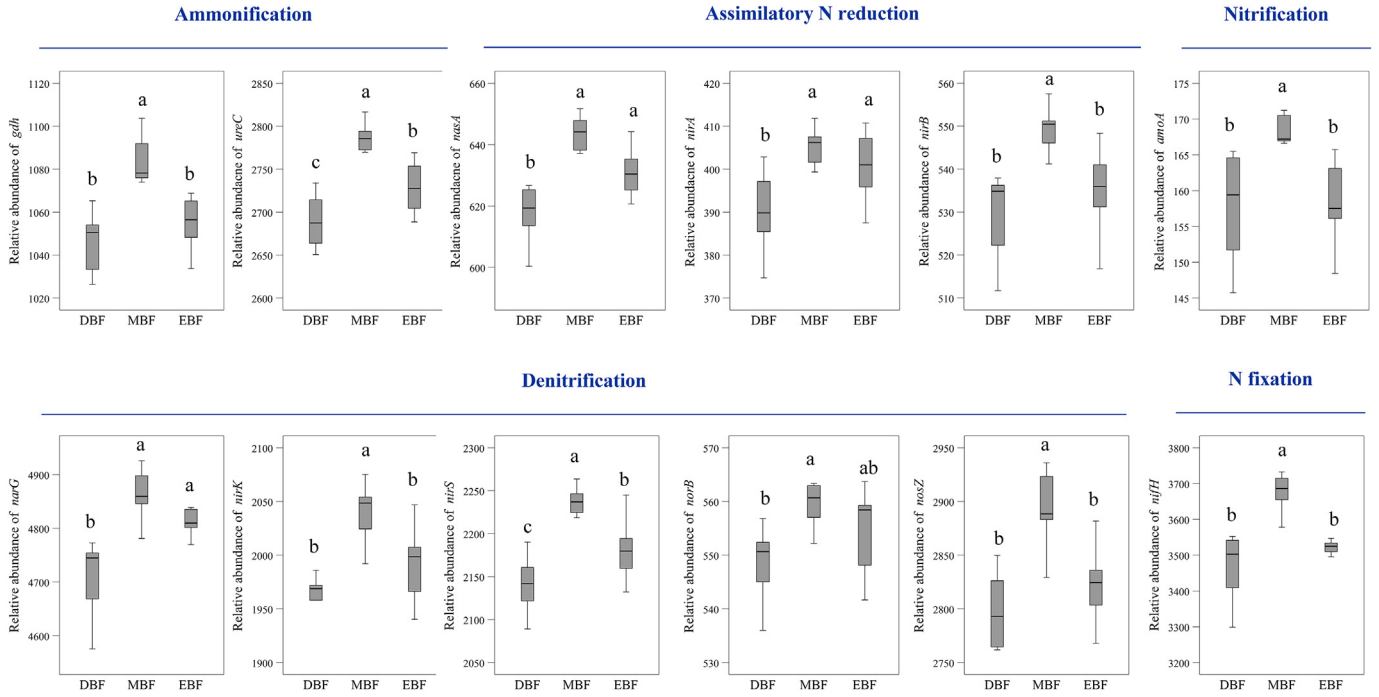

Fig. 3. Comparison of microbial functional genes for N cycling among forests. DBF: the deciduous broad-leaved forest. MBF: the mixed deciduous-evergreen broad-leaved forest. EBF: the evergreen broad-leaved forest. Letters including "a" "b" and "c" above bars indicate significant difference ($P < 0.05$) among forests.

oxide reductase ($N_2O \rightarrow N_2$), were more abundant in the MBF than in others (Fig. 3, $P < 0.05$). Among the three forests, relative abundances of *ureC*, *nasA* encoding nitrate reductase for assimilatory N reduction ($NO_3^- \rightarrow NO_2^-$), *nirA* encoding nitrite reductase for assimilatory N reduction ($NO_2^- \rightarrow NH_4^+$), *narG* encoding nitrate reductase for denitrification ($NO_3^- \rightarrow NO_2^-$), *nirS*, and *norB* encoding nitric oxide reductase for denitrification ($NO \rightarrow N_2O$) were the lowest in the DBF (Fig. 3, $P < 0.05$).

3.2.4. P cycling genes

We detected significantly higher relative abundances of P cycling genes in the MBF than in other forests ($P < 0.001$, $F = 32.59$), including the phytase gene for the step-wise removal of phosphate from phytate, the *ppk* encoding polyphosphate kinase for the formation of polyphosphate from ATP, and the *ppx* encoding exopolyphosphatase for the degradation of polyphosphate. Relative abundances of *ppk* and *ppx* were the lowest in the DBF (Fig. S2, $P < 0.05$).

3.2.5. S cycling genes

We detected significantly higher relative abundances of S cycling genes in the MBF than in other forests ($P < 0.001$, $F = 27.48$), including the *aprA* encoding adenosine-5′-phosphosulfate reductase for sulfate reduction, the *cysJ* encoding sulphite reductase flavoprotein, the *dsrA* and *dsrB* encoding dissimilatory sulfate reductase, and the *soxY* encoding sulfur covalently binding protein for sulfur oxidation. Relative abundances of *cysJ* and *soxY* were the lowest in the DBF (Fig. S3, $P < 0.05$).

3.3. Environmental indicators of soil microbial functional structure

Partial Mantel tests demonstrated that soil microbial functional gene structure of the DBF was significantly related to soil total S ($r_M = 0.450$, $P = 0.041$), that of the MBF was significantly related to soil organic C ($r_M = 0.416$, $P = 0.027$) and plant available P ($r_M = 0.378$, $P = 0.034$), and that of the EBF was significantly related to soil pH ($r_M = 0.425$, $P = 0.006$) and total K ($r_M = 0.442$, $P = 0.038$) (Table 2). None of the plant-related variables were revealed as significant indicators of soil microbial functional gene composition (Table 2). In accordance, the MRM results also verified that edaphic variables ($P < 0.01$) were more important than plant-related ones ($P = 0.86$) in predicting soil microbial functional structure (Table 3).

Table 2
Results of the partial Mantel test between microbial functional gene composition and environmental variables. DBF: the deciduous broad-leaved forest. MBF: the mixed deciduous-evergreen broad-leaved forest. EBF: the evergreen broad-leaved forest. Bold values indicate significance at the $P < 0.05$ level.

Environmental variables	DBF		MBF		EBF	
	r_M	*P*	r_M	*P*	r_M	*P*
Plant-related variables						
dIVI	−0.057	0.350	−0.329	0.976	0.282	0.178
Shannon-Wiener index	−0.016	0.410	−0.346	0.986	0.120	0.290
Richness	0.143	0.186	−0.225	0.829	0.110	0.228
Pielou's evenness	−0.140	0.670	−0.367	0.997	0.027	0.441
All	−0.003	0.457	−0.204	0.831	0.111	0.236
Edaphic variables						
Soil pH	0.045	0.308	0.084	0.359	0.425	**0.006**
Organic carbon (C)	0.205	0.196	0.416	**0.027**	−0.542	0.986
Total nitrogen (N)	0.271	0.208	0.389	0.058	−0.536	0.996
Total potassium (K)	0.003	0.321	−0.066	0.535	0.442	**0.038**
Total phosphorus (P)	0.294	0.133	0.311	0.107	0.186	0.225
Total sulfur (S)	0.450	**0.041**	0.250	0.076	0.184	0.211
NH_4^+-N	−0.110	0.640	0.166	0.245	0.013	0.446
NO_3^--N	−0.189	0.788	0.230	0.089	−0.106	0.735
Alkali-hydrolysable N	0.167	0.268	0.376	0.056	−0.526	0.985
Plant available P	−0.194	0.757	0.378	**0.034**	−0.038	0.541
Fe^{3+}	−0.010	0.402	−0.074	0.617	0.306	0.077
All	0.359	**0.049**	0.420	**0.025**	−0.107	0.645

Table 3
Results of the MRM (multiple regression on distance matrices) between microbial functional gene composition and environmental variables. Plant-related variables include dIVI, Shannon-Wiener index, richness, and Pielou's evenness. Edaphic variables include pH, organic C, total N, total K, total P, total S, NH_4^+-N, NO_3^--N, alkali-hydrolysable N, plant available P, and Fe^{3+}. Bold values indicate significance at the $P < 0.01$ level.

	Coefficient	*P*-value	F-value of MRM model (*P*-value)
Plant-related variables	0.79	0.86	24.67 (< **0.01**)
Edaphic variables	10.47	< **0.01**	

3.4. Network topological characteristics

Functional molecule ecological networks showed clearly different topological properties among forests (Table 4). Compared to networks of the DBF and the EBF, networks of the MBF were more complex and intensive, which contained more nodes and edges and had higher average connectivity and average clustering coefficient (Figs. 4, 5 & S4–S6). For example, with the threshold of 0.980, the C decomposition network of MBF had a larger node number (1978) than that of the DBF (1136) and EBF (1053), and the edge number of MBF (3944) was 4–5 times larger than that of the DBF (877) and EBF (790) (Fig. 4 & Table 4). Average connectivity of the C decomposition network of MBF (3.988) was 2–3 times larger than that of the DBF (1.544) and EBF (1.500). Average

Table 4
Topological characteristics of forest-specific networks based on microbial functional genes for nutrient cycling. DBF: the deciduous broad-leaved forest. MBF: the mixed deciduous-evergreen broad-leaved forest. EBF: the evergreen broad-leaved forest.

Network topological characteristics	DBF	MBF	EBF
C decomposition			
Threshold	0.980	0.980	0.980
Total nodes	1136	1978	1053
Total edges	877	3944	790
R^2 of power-law	0.944	0.886	0.887
Average connectivity	1.544	3.988	1.500
Average clustering coefficient	0.137	0.224	0.091
Modularity	0.990	0.822	0.983
C fixation			
Threshold	0.960	0.960	0.960
Total nodes	1172	1636	1174
Total edges	1112	4449	1064
R^2 of power-law	0.888	0.817	0.891
Average connectivity	1.898	5.439	1.813
Average clustering coefficient	0.192	0.329	0.177
Modularity	0.970	0.759	0.969
N cycling			
Threshold	0.960	0.960	0.960
Total nodes	1449	1982	1384
Total edges	1438	7286	1392
R^2 of power-law	0.889	0.823	0.912
Average connectivity	1.985	7.352	2.012
Average clustering coefficient	0.204	0.360	0.190
Modularity	0.971	0.710	0.952
P cycling			
Threshold	0.920	0.920	0.920
Total nodes	610	735	547
Total edges	770	2813	637
R^2 of power-law	0.848	0.735	0.856
Average connectivity	2.525	7.654	2.329
Average clustering coefficient	0.205	0.336	0.200
Modularity	0.906	0.639	0.875
S cycling			
Threshold	0.960	0.960	0.960
Total nodes	658	1041	624
Total edges	563	2382	486
R^2 of power-law	0.943	0.841	0.926
Average connectivity	1.711	4.576	1.558
Average clustering coefficient	0.143	0.319	0.157
Modularity	0.962	0.769	0.983

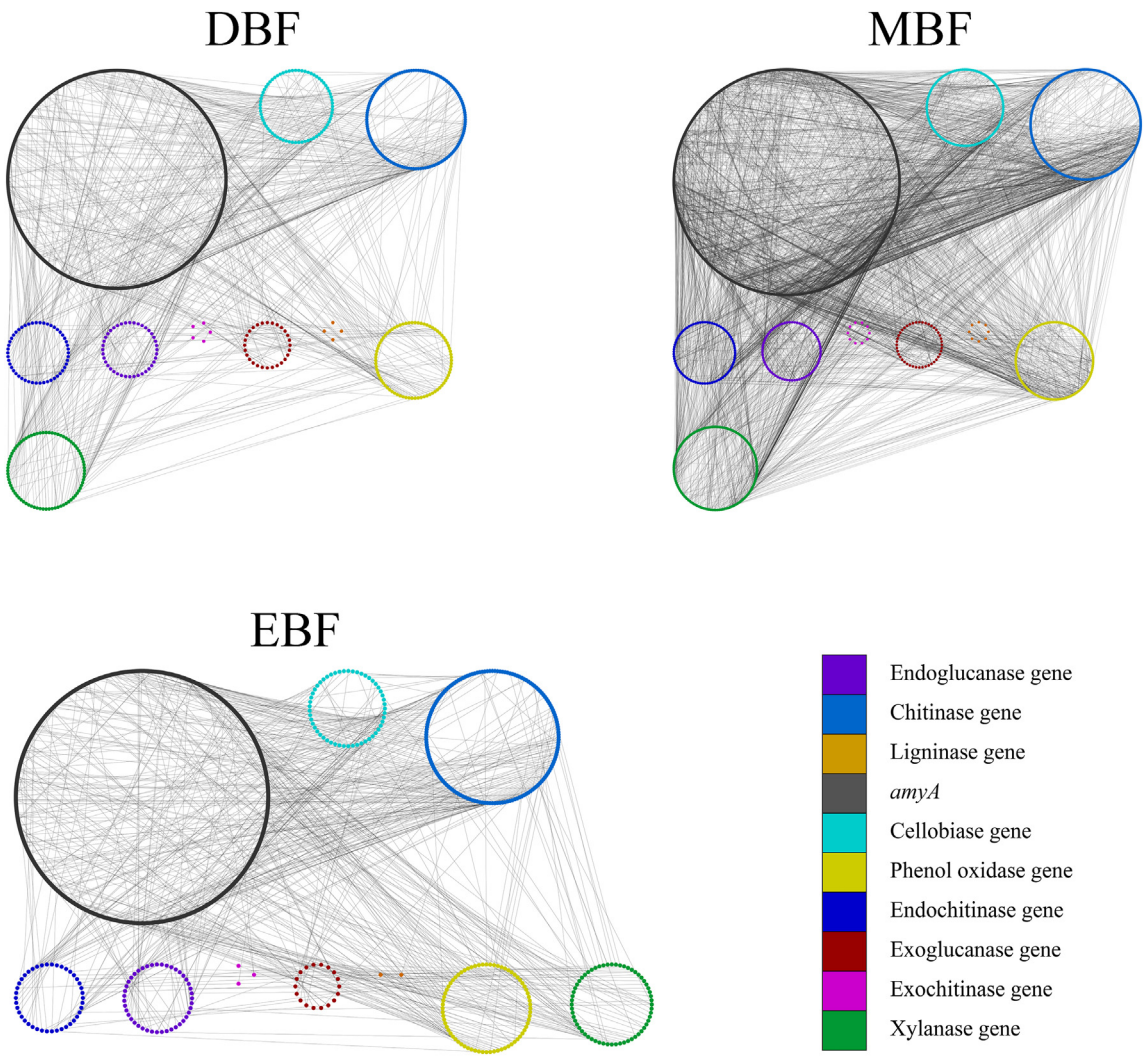

Fig. 4. Topology of forest-specific networks based on microbial functional genes for C decomposition. DBF: the deciduous broad-leaved forest. MBF: the mixed deciduous-evergreen broad-leaved forest. EBF: the evergreen broad-leaved forest. Each dot indicates a node and each line indicates an edge. Nodes are separated by genes, which are indicated by different colors.

clustering coefficient of the C decomposition network of MBF (0.224) was 1–3 times larger than that of the DBF (0.137) and EBF (0.091) (Fig. 4 & Table 4). Similar topological patterns were also detected for C fixation networks (Fig. S4), N cycling networks (Fig. 5), P cycling networks (Fig. S5), and S cycling networks (Fig. S6).

4. Discussion

Soil microbial taxonomic structure has been widely investigated in numerous studies (Cheng et al., 2020; He et al., 2012; Hu et al., 2014), while only a few have attempted to integrate microbial taxonomy with function (Mendes et al., 2014; Navarrete et al., 2015; Pérez-Jaramillo et al., 2019). In the present study, we investigated patterns of soil microbial functional structure in three types of subtropical broad-leaved forests (i.e., DBF, MBF, and EBF), which were indicated by functional gene quantification via GeoChip. Although caution is required when interpreting the functional gene data due to the lack of enzyme activity measurements, GeoChip has been successfully used in a range of ecosystem types (He et al., 2007; Ma et al., 2019; Wang et al., 2017). As expected, significantly different patterns of functional structure were observed among forests (Fig. 1a & Table 1), indicating different soil microbial functional capabilities of the three vegetation types. In our previous study, higher taxonomic diversity of soil bacteria and archaea communities (based on 16S rRNA gene sequencing) was observed in the DBF than in the MBF and the EBF (Cheng et al., 2020). However, the DBF did not show the highest functional gene diversity in our present study (Fig. 1b & c). The inconsistency between taxonomic diversity and functional diversity probably means a high degree of microbial functional redundancy (i.e., different microbial taxa play the same functional role in ecosystems) (Loreau, 2004) in the DBF. Higher functional β-diversity in the DBF and EBF (Fig. 1d) indicated higher site-to-site differentiation of soil microbial functions below the deciduous stands and evergreen ones (Socolar et al., 2016). Whereas, lower functional β-diversity in the MBF indicated higher site-to-site functional homogenization below the mixed stands (Socolar et al., 2016).

Compared to the DBF and the EBF, higher functional gene diversity (Fig. 1b & c) and gene abundances for nutrient cycling processes (Figs. 2, 3 & S1–S3) of the MBF indicated that soil microbial communities below the mixed deciduous-evergreen stands had higher functional capabilities in more ecological processes. A possible explanation is litter mixing effects, i.e., litter from different vegetation types could promote the microbe-mediated decomposition and nutrient turnover, which has been observed in several studies (Hu et al., 2006; Liu et al., 2016; Wang et al., 2019; Wang et al., 2020). For example, a previous study showed that mixed litter from deciduous species and evergreen ones accelerated litter decomposition in a Chinese subtropical forest (Liu et al., 2016). In addition, mixed litter from coniferous species and broad-leaved ones promoted degradative enzyme activities and functional gene abundances of specific microbial taxa (Wang et al., 2020). Most microbial functional genes in association with C, N, P, and S cycling

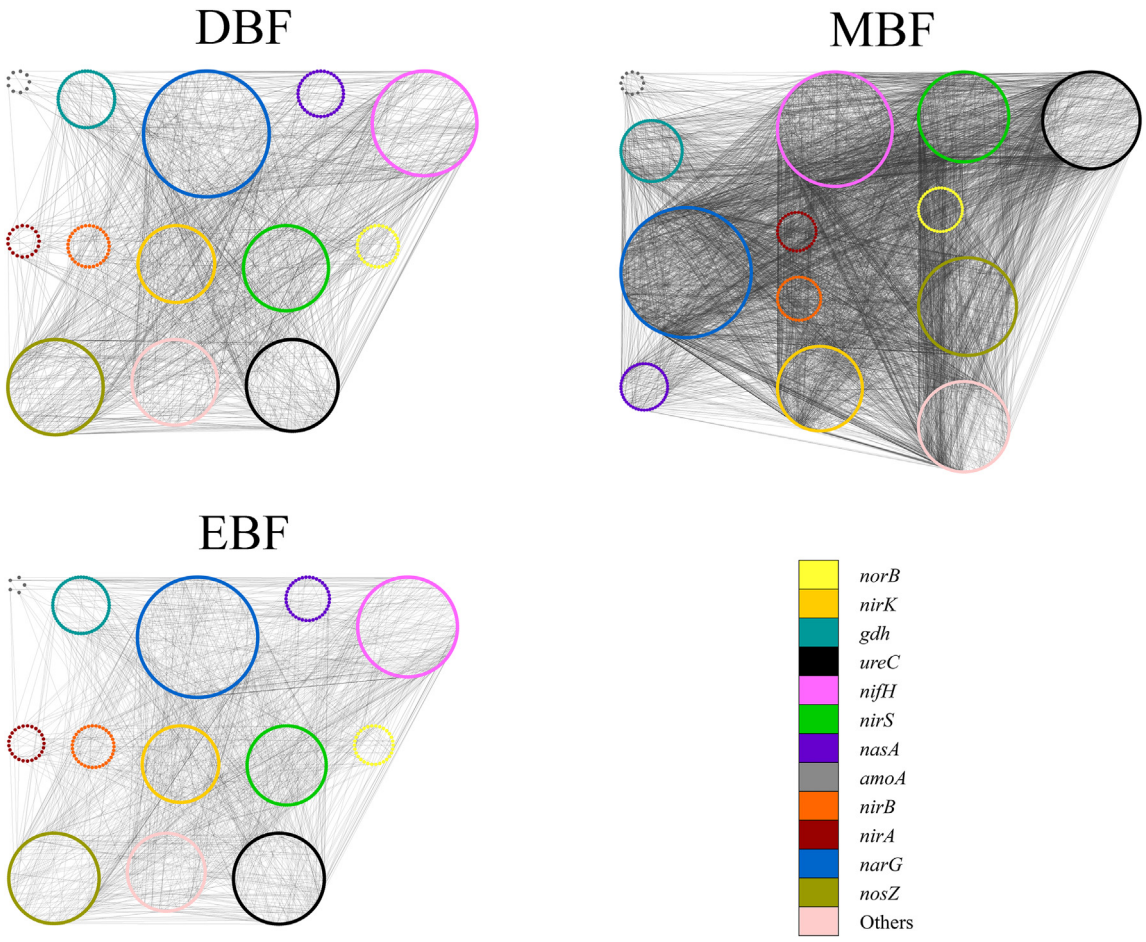

Fig. 5. Topology of forest-specific networks based on microbial functional genes for N cycling. DBF: the deciduous broad-leaved forest. MBF: the mixed deciduous-evergreen broad-leaved forest. EBF: the evergreen broad-leaved forest. Each dot indicates a node and each line indicates an edge. Nodes are separated by genes, which are indicated by different colors.

were significantly higher in the MBF than in the other two vegetation types, but the MBF did not exhibit significantly higher or lower corresponding soil nutrients (Table S1). A possible reason is that higher abundances of functional genes measured by GeoChip only indicate higher functional capabilities or potentials but not higher microbial activities in nutrient cycling processes (He et al., 2007). According to a previous study showing that higher precipitation could enhance the abundance of microbial enzymes for C decomposition (Ren et al., 2017), we suspected that higher MAP (1527.1 mm of the MBF vs. 1009.5 mm of the DBF, 1465.6 mm of the EBF) might be another explanation of the higher microbial capability in C decomposition in the MBF. Unfortunately, we could not evaluate the effects of MAP in this study because our MAP data were vegetation-type specific instead of sampling-plot specific, i.e., each vegetation type has only one MAP regardless of nine sampling plots. Additional studies are needed to interpret the relationship of climatic variables and soil microbial functional structure.

Network analysis is a convenient way to reveal potential microbial interactions. Topological properties of the constructed networks could somewhat reflect whole-network differences among different natural or experimental settings, which has been justified by plenty of recent articles (Barberán et al., 2012; Cordero and Datta, 2016; de Vries et al., 2018). In this study, higher average connectivity and average clustering coefficient of networks of the MBF (Figs. 4, 5 & S4–S6; Table 4) indicated that soil microbial communities under this vegetation type could function more closely in nutrient cycling processes and be more resistant to environmental disturbance (de Vries et al., 2018). This finding also implies that forest restoration can benefit from the co-existence of deciduous plant species and evergreen ones. However, one should always be careful when interpreting microbial ecological networks since most true microbial interactions remain largely intractable experimentally, except symbionts. Moreover, we should bear in mind that the small sampling size of networks (9 replicates) suggests that we may run the risk of getting spurious correlations.

Variation of microbial functional gene structure is often accompanied by variation of both plant and soil properties across a range of ecosystems (Hu et al., 2019; Kandeler et al., 2006; Yang et al., 2014). However, in contrast to our expectation, effects of plant-related variables on microbial functional gene structure were statistically insignificant (Tables 2 & 3). This result indicated that plant properties, especially vegetation type and plant diversity, are not good to inform soil microbial functional structure in SBFs, regardless of the obvious trophic linkages between plants (producers) and microorganisms (decomposers). Similar findings were found in two previous studies that also targeted on soil microbial functional structure of Chinese subtropical forests (Ding et al., 2015a,b). Owing to the limited measurements of plant-related variables, we should bear in mind that this study only evaluated the effects of plant community as a whole, rather than individual plant species. Other plant-related variables, e.g., plant litter, dominant tree species, plant genotype, and plant phylogenetic diversity, have been reported to impact soil microbial communities (Berg and Smalla, 2009; Prescott and Grayston, 2013; Purahong et al., 2016; Schulz et al., 2012), and should be concluded in future studies to better interpret plant effects.

As expected, edaphic variables, including total S, organic C, plant available P, soil pH, and total K, were revealed as better indicators of soil microbial functional capabilities in SBFs than plant-related variables (Tables 2 & 3). These results indicated that soil properties including soil pH and nutrient content, rather than plant properties, strongly affected

soil microbial functional structure in SBFs. Soil microbial functional structures under different vegetation types had different environmental indicators (Table 2), implying different mechanisms underlying their formation. For example, soil total S, which was approximately two times lower in the DBF than in the other two vegetation types (Table S1), was the indicator of microbial functional structure of the DBF (Table 2). These results indicated that soil total S was more limited in the DBF, and such deficiency could strongly influence soil microbial community at the functional gene level. Soil S availability is determined by both microorganisms and plants, as microorganisms mineralize organic S and uptake S for biomass, and plants provide litter containing organic S into soil and uptake S for growth and production (Kumar et al., 2018). According to a previous survey of forests, plant leaf S content of DBFs (2.7 ± 0.5 mg g^{-1}) is significantly higher than that of MBFs (1.0 ± 0.1 mg g^{-1}) and EBFs (0.8 ± 0.1 mg g^{-1}) (Wu et al., 2017). Therefore, it is highly likely that lower soil total S in the DBF results from larger S uptake of plants. Likewise, soil pH and soil total K, both significantly higher in the EBF than in others (Table S1), strongly influenced the microbial functional structure under the EBF (Table 2). It is not surprising to detect the importance of soil pH since this edaphic variable has been revealed as a driving force of soil microbial communities at the global scale, especially bacterial communities (Fierer and Jackson, 2006). However, the importance of soil total K suggested that K element, which has long been understudied in comparison with N and P elements (Tripler et al., 2006), may play critical roles in maintaining soil microbial functional structure in forest ecosystems.

The predominant effects of edaphic variables in shaping soil microbial functional structure have also been demonstrated previously (Ding et al., 2015a,b). For example, quantity and quality of soil organic matters were revealed as the best indicators of soil microbial functional structure in two subtropical forests in Shennongjia Mountain (Ding et al., 2015b). Plant community, soil, and microbial community form a complex system with a variety of microhabitats and physicochemical gradients (Torsvik and Øvreås, 2002), and one particularly intriguing question is to what degree plant community influences microbial community (Prescott and Grayston, 2013). From the perspective of functional structure, our results indicated that plant and microbial communities were not directly linked but linked through soil habitats. Soil served as a bridge between these two ecosystem components: Accumulated nutrient resources in the forms of litter and root exudates are released by plant communities into the soil, which change soil physicochemical properties (such as soil pH and nutrient content); Accordingly, microbial communities change the functional structure to adapt soil habitats and participate a range of nutrient cycling processes.

5. Conclusions

This study provides a direct quantification of microbial functional gene profiles in three typical vegetation types of SBFs (i.e., a DBF, a MBF, and an EBF). In conclusion, we found significantly different soil microbial functional traits including composition, diversity, relative abundance, and network topology of functional genes among forests. To our surprise, plant-related variables (i.e., vegetation type and diversity) were not good indicators of soil microbial functional structure in SBFs. Instead, edaphic variables (i.e., soil pH and nutrient contents) were identified as better indicators of soil microbial functional structure. This study highlights the importance of soil properties and improves our understanding of patterns and mechanisms of soil microbial functional structure in SBFs.

CRediT authorship contribution statement

Yuguang Zhang conceived the ideas and designed the methodology; Jing Cong collected the data; Yuguang Zhang, Jing Cong, and Jingjing Yu did GeoChip hybridization and soil nutrient measurements; Jingmin Cheng and Zhongjie Han analyzed the data; Jingming Cheng wrote the first draft of the manuscript. Yuguang Zhang and Mengxin Zhao revised the manuscript. All authors contributed to the manuscript and gave final approval for publication.

Data accession

The GeoChip data and the environmental data are accessible in the Gene Expression Omnibus (GEO) database with the accession ID "GSE165723" (https://www.ncbi.nlm.nih.gov/geo/query/acc.cgi?acc=GSE165723).

Declaration of competing interest

The authors declare that they have no known competing financial interests or personal relationships that could have appeared to influence the work reported in this paper.

Acknowledgments

We thank three anonymous reviewers for insightful suggestions to make this paper greatly improved. This research was financed by the National Natural Science Foundation of China (No. 31670614 and No. 41601583), the Public Welfare Project of the National Scientific Research Institution (No. CAFYBB2018SZ005), the Strategic Priority Research Program of the Chinese Academy of Sciences (No. XDB15010302), the China Postdoctoral Science Foundation of Mengxin Zhao (No. 2017M620743), and the National Biological Specimens and Resources Sharing Platform in Nature Reserve (No. 2005DKA21404).

Appendix A. Supplementary data

Supplementary data to this article can be found online at https://doi.org/10.1016/j.scitotenv.2021.145630.

References

Antúnez, I., Retamosa, E.C., Villar, R., 2001. Relative growth rate in phylogenetically related deciduous and evergreen woody species. Oecologia 128, 172–180.
Bai, S., Li, J., He, Z., Nostrand, J.D., Tian, Y., Lin, G., et al., 2013. GeoChip-based analysis of the functional gene diversity and metabolic potential of soil microbial communities of mangroves. Applied Microbiology Biotechnology 97, 7035–7048.
Bao, S., 2000. Soil and Agricultural Chemistry Analysis. Agriculture Publication, Beijing.
Barberán, A., Bates, S.T., Casamayor, E.O., Fierer, N., 2012. Using network analysis to explore co-occurrence patterns in soil microbial communities. The ISME Journal 6, 343–351.
Berg, G., Smalla, K., 2009. Plant species and soil type cooperatively shape the structure and function of microbial communities in the rhizosphere. FEMS Microbiol. Ecol. 68, 1–13.
Cheng, J., Zhao, M., Cong, J., Qi, Q., Xiao, Y., Cong, W., et al., 2020. Soil pH exerts stronger impacts than vegetation type and plant diversity on soil bacterial community composition in subtropical broad-leaved forests. Plant Soil 450, 273–286.
Chodak, M., Klimek, B., Azarbad, H., Jazwa, M., 2015. Functional diversity of soil microbial communities under Scots pine, Norway spruce, silver birch and mixed boreal forests. Pedobiologia 58 (2–3), 81–88.
Cordero, O.X., Datta, M.S., 2016. Microbial interactions and community assembly at microscales. Curr. Opin. Microbiol. 31, 227–234.
Curtis, J., Mcintosh, R., 1951. An upland forest continuum in the prairie-forest border region of Wisconsin. Ecology 32, 476–496.
Dai, Z., Liu, G., Chen, H., Chen, C., Wang, J., Ai, S., et al., 2020. Long-term nutrient inputs shift soil microbial functional profiles of phosphorus cycling in diverse agroecosystems. The ISME Journal 14, 757–770.
De Graaff, M.A., Classen, A.T., Castro, H.F., Schadt, C.W., 2010. Labile soil carbon inputs mediate the soil microbial community composition and plant residue decomposition rates. New Phytol. 188, 1055–1064.
de Vries, F.T., Griffiths, R.I., Bailey, M., Craig, H., Girlanda, M., Gweon, H.S., et al., 2018. Soil bacterial networks are less stable under drought than fungal networks. Nat. Commun. 9, 3033.
Deng, Y., Jiang, Y., Yang, Y., He, Z., Luo, F., Zhou, J., 2012. Molecular ecological network analyses. BMC Bioinformatics 13, 113.
Ding, J., Zhang, Y., Deng, Y., Cong, J., Lu, H., Sun, X., et al., 2015a. Integrated metagenomics and network analysis of soil microbial community of the forest timberline. Sci. Rep. 5, 7994.
Ding, J., Zhang, Y., Wang, M., Sun, X., Cong, J., Deng, Y., et al., 2015b. Soil organic matter quantity and quality shape microbial community compositions of subtropical broadleaved forests. Mol. Ecol. 24, 5175–5185.

Ettema, C.H., Wardle, D.A., 2002. Spatial soil ecology. Trends in Ecology and Evolution 17, 177–183.
Fierer, N., Jackson, R.B., 2006. The diversity and biogeography of soil bacterial communities. Proc. Natl. Acad. Sci. U. S. A. 103, 626–631.
Harter, J., Krause, H.-M., Schuettler, S., Ruser, R., Fromme, M., Scholten, T., et al., 2014. Linking N_2O emissions from biochar-amended soil to the structure and function of the N-cycling microbial community. The ISME Journal 8, 660–674.
He, Z., Gentry, T.J., Schadt, C.W., Wu, L., Liebich, J., Chong, S.C., et al., 2007. GeoChip: a comprehensive microarray for investigating biogeochemical, ecological and environmental processes. The ISME Journal 1, 67–77.
He, Z., Piceno, Y., Deng, Y., Xu, M., Lu, Z., DeSantis, T., et al., 2012. The phylogenetic composition and structure of soil microbial communities shifts in response to elevated carbon dioxide. The ISME Journal 6, 259–272.
Hu, Y., Wang, S., Zeng, D., 2006. Effects of single Chinese fir and mixed leaf litters on soil chemical, microbial properties and soil enzyme activities. Plant Soil 282, 379–386.
Hu, Y., Xiang, D., Veresoglou, S.D., Chen, F., Chen, Y., Hao, Z., et al., 2014. Soil organic carbon and soil structure are driving microbial abundance and community composition across the arid and semi-arid grasslands in northern China. Soil Biol. Biochem. 77, 51–57.
Hu, Y., Zhang, Z., Huang, L., Qi, Q., Liu, L., Zhao, Y., et al., 2019. Shifts in soil microbial community functional gene structure across a 61-year desert revegetation chronosequence. Geoderma 347, 126–134.
Kandeler, E., Deiglmayr, K., Tscherko, D., Bru, D., Philippot, L., 2006. Abundance of narG, nirS, nirK, and nosZ genes of denitrifying bacteria during primary successions of a glacier foreland. Applied Environmental Microbiology 72, 5957–5962.
Kumar, U., Panneerselvam, P., Gupta, V.V.S.R., Manjunath, M., Priyadarshinee, P., Sahoo, A., et al., 2018. Diversity of sulfur-oxidizing and sulfur-reducing microbes in diverse ecosystems. In: Adhya, T.K., Lal, B., Mohapatra, B., Paul, D., Das, S. (Eds.), Advances in Soil Microbiology: Recent Trends and Future Prospects: Volume 1: Soil-Microbe Interaction. Springer Singapore, Singapore, pp. 65–89.
Lamb, E.G., Kennedy, N., Siciliano, S.D., 2011. Effects of plant species richness and evenness on soil microbial community diversity and function. Plant Soil 338, 483–495.
Levy-Booth, D.J., Prescott, C.E., Grayston, S.J., 2014. Microbial functional genes involved in nitrogen fixation, nitrification and denitrification in forest ecosystems. Soil Biol. Biochem. 75, 11–25.
Liu, C., Liu, Y., Guo, K., Zhao, H., Qiao, X., Wang, S., et al., 2016. Mixing litter from deciduous and evergreen trees enhances decomposition in a subtropical karst forest in southwestern China. Soil Biol. Biochem. 101, 44–54.
Loreau, M., 2004. Does functional redundancy exist? Oikos 104, 606–611.
Lu, Z., Deng, Y., Van Nostrand, J.D., He, Z., Voordeckers, J., Zhou, A., et al., 2012. Microbial gene functions enriched in the Deepwater Horizon deep-sea oil plume. The ISME Journal 6, 451–460.
Lynn, T.M., Ge, T., Yuan, H., Wei, X., Wu, X., Xiao, K., et al., 2017. Soil carbon-fixation rates and associated bacterial diversity and abundance in three natural ecosystems. Microb. Ecol. 73, 645–657.
Ma, X., Zhang, Q., Zheng, M., Gao, Y., Yuan, T., Hale, L., et al., 2019. Microbial functional traits are sensitive indicators of mild disturbance by lamb grazing. The ISME Journal 13, 1370–1373.
Mendes, L.W., Kuramae, E.E., Navarrete, A.A., Van Veen, J.A., Tsai, S.M., 2014. Taxonomical and functional microbial community selection in soybean rhizosphere. The Isme Journal 8, 1577–1587.
Navarrete, A.A., Tsai, S.M., Mendes, L.W., Faust, K., Hollander, M.D., Cassman, N.A., et al., 2015. Soil microbiome responses to the short-term effects of Amazonian deforestation. Mol. Ecol. 24, 2433–2448.
Pearse, I.S., Cobb, R.C., Karban, R., 2014. The phenology–substrate-match hypothesis explains decomposition rates of evergreen and deciduous oak leaves. J. Ecol. 102, 28–35.
Pérez-Jaramillo, J.E., Hollander, M.D., Ramírez, C.A., Mendes, R., Raaijmakers, J.M., Carrión, V.J., 2019. Deciphering rhizosphere microbiome assembly of wild and modern common bean (Phaseolus vulgaris) in native and agricultural soils from Colombia. Microbiome 7, 114.
Pérez-Suárez, M., Arredondo-Moreno, J.T., Huber-Sannwald, E., Vargas-Hernández, J.J., 2009. Production and quality of senesced and green litterfall in a pine–oak forest in central-northwest Mexico. For. Ecol. Manag. 258, 1307–1315.
Prescott, C.E., Grayston, S.J., 2013. Tree species influence on microbial communities in litter and soil: current knowledge and research needs. For. Ecol. Manag. 309, 19–27.
Purahong, W., Durka, W., Fischer, M., Dommert, S., Schöps, R., Buscot, F., et al., 2016. Tree species, tree genotypes and tree genotypic diversity levels affect microbe-mediated soil ecosystem functions in a subtropical forest. Sci. Rep. 6, 36672.
Ren, C., Zhao, F., Shi, Z., Chen, J., Han, X., Yang, G., et al., 2017. Differential responses of soil microbial biomass and carbon-degrading enzyme activities to altered precipitation. Soil Biol. Biochem. 115, 1–10.
Schulz, Giebler, Chatzinotas, Wick, L.Y., Fetzer, et al., 2012. Plant litter and soil type drive abundance, activity and community structure of alkB harbouring microbes in different soil compartments. The ISME Journal 6 (9), 1763–1774.
Socolar, J.B., Gilroy, J.J., Kunin, W.E., Edwards, D.P., 2016. How should beta-diversity inform biodiversity conservation? Trends in Ecology and Evolution 31, 67–80.
Takashima, T., Hikosaka, K., Hirose, T., 2004. Photosynthesis or persistence: nitrogen allocation in leaves of evergreen and deciduous Quercus species. Plant Cell Environ. 27, 1047–1054.
Torsvik, V., Øvreås, L., 2002. Microbial diversity and function in soil: from genes to ecosystems. Curr. Opin. Microbiol. 5, 240–245.
Tripler, C.E., Kaushal, S.S., Likens, G.E., Todd, Walter M., 2006. Patterns in potassium dynamics in forest ecosystems. Ecol. Lett. 9, 451–466.
Ulrich, G., Martino, D., Burger, K., Routh, J., Grossman, E., Ammerman, J., et al., 1998. Sulfur cycling in the terrestrial subsurface: commensal interactions, spatial scales, and microbial heterogeneity. Microb. Ecol. 36, 141–151.
Wang, F., Zhou, H., Meng, J., Peng, X., Jiang, L., Sun, P., et al., 2009. GeoChip-based analysis of metabolic diversity of microbial communities at the Juan de Fuca Ridge hydrothermal vent. Proc. Natl. Acad. Sci. U. S. A. 106, 4840–4845.
Wang, M., Wang, S., Wu, L., Xu, D., Lin, Q., Hu, Y., et al., 2016. Evaluating the lingering effect of livestock grazing on functional potentials of microbial communities in Tibetan grassland soils. Plant Soil 407, 385–399.
Wang, H., Yu, L., Zhang, Z., Liu, W., Chen, L., Cao, G., et al., 2017. Molecular mechanisms of water table lowering and nitrogen deposition in affecting greenhouse gas emissions from a Tibetan alpine wetland. Glob. Chang. Biol. 23, 815–829.
Wang, W., Chen, D., Sun, X., Zhang, Q., Koide, R.T., Insam, H., et al., 2019. Impacts of mixed litter on the structure and functional pathway of microbial community in litter decomposition. Appl. Soil Ecol. 144, 72–82.
Wang, W., Chen, D., Zhang, Q., Sun, X., Zhang, S., 2020. Effects of mixed coniferous and broad-leaved litter on bacterial and fungal nitrogen metabolism pathway during litter decomposition. Plant Soil 1–17.
Wang, Q., Xiao, J., Ding, J., Zou, T., Zhang, Z., Liu, Q., et al., 2021. Differences in root exudate inputs and rhizosphere effects on soil N transformation between deciduous and evergreen trees. Plant Soil 458, 277–289.
Wu, Y., Liu, H., Song, Z., Yang, X., Li, Z., Hao, Q., et al., 2017. Ecological stoichiometry of nitrogen, phosphorous, and sulfur in China's forests. Acta Geochimica 36, 525–530.
Xue, K., Yuan, M.M., Shi, Z.J., Qin, Y., Deng, Y., Cheng, L., et al., 2016. Tundra soil carbon is vulnerable to rapid microbial decomposition under climate warming. Nat. Clim. Chang. 6, 595–600.
Yang, Y., Gao, Y., Wang, S., Xu, D., Yu, H., Wu, L., et al., 2014. The microbial gene diversity along an elevation gradient of the Tibetan grassland. The ISME Journal 8, 430–440.
Yergeau, E., Kang, S., He, Z., Zhou, J., Kowalchuk, G.A., 2007. Functional microarray analysis of nitrogen and carbon cycling genes across an Antarctic latitudinal transect. The ISME Journal 1, 163–179.
Yu, G., Chen, Z., Piao, S., Peng, C., Ciais, P., Wang, Q., et al., 2014. High carbon dioxide uptake by subtropical forest ecosystems in the East Asian monsoon region. Proc. Natl. Acad. Sci. U. S. A. 111, 4910–4915.
Zak, D.R., Holmes, W.E., White, D.C., Peacock, A.D., Tilman, D., 2003. Plant diversity, soil microbial communities, and ecosystem function: are there any links? Ecology 84, 2042–2050.
Zhou, J., Deng, Y., Luo, F., He, Z., Yang, Y., 2011. Phylogenetic molecular ecological network of soil microbial communities in response to elevated CO_2. MBio 2 e00122-11.
Zimmerman, N., Izard, J., Klatt, C., Zhou, J., Aronson, E., 2016. The unseen world: environmental microbial sequencing and identification methods for ecologists. Front. Ecol. Environ. 12, 224–231.